

Semiclassical theory for quantum quenches in finite transverse Ising chains

Heiko Rieger^{1,*} and Ferenc Iglói^{2,3,†}

¹*Theoretische Physik, Universität des Saarlandes, DE-66041 Saarbrücken, Germany*

²*Research Institute for Solid State Physics and Optics, HU-1525 Budapest, P.O. Box 49, Hungary*

³*Institute of Theoretical Physics, Szeged University, HU-6720 Szeged, Hungary*

(Received 26 June 2011; published 19 October 2011)

We present a quantitative semiclassical theory for the nonequilibrium dynamics of transverse Ising chains after quantum quenches, in particular, sudden changes of the transverse field strength. We obtain accurate predictions for the quench-dependent relaxation times and correlation lengths, and also about the recurrence times and quasiperiodicity of time-dependent correlations in finite systems with open or periodic boundary conditions. We compare the quantitative predictions of our semiclassical theory (local magnetization, equal-time bulk-bulk and surface-to-bulk correlations, and bulk autocorrelations) with the results from exact free-fermion calculations, and discuss the range of applicability of the semiclassical theory and possible generalizations and extensions.

DOI: [10.1103/PhysRevB.84.165117](https://doi.org/10.1103/PhysRevB.84.165117)

PACS number(s): 64.70.Tg, 05.70.Ln, 75.10.Pq, 75.40.Gb

I. INTRODUCTION

The nonequilibrium quantum relaxation in many-body systems has gained increased interest over the recent years, not least because trapped cold-atom systems made its experimental study possible. In principle, one asks for the fate of an initial state that is not an eigenstate of the Hamiltonian under the time evolution according to the Schrödinger equation. A straightforward method to prepare such an initial state is the instantaneous change of a global or local parameter of the system such as an external field or the interaction strength, denoted as a quantum quench or simply quench. Important issues of interest are then as follows: (1) Is there an asymptotic stationary state, what are its characteristics, is it describable by a general Gibbs ensemble (i.e., does the system thermalize after a quench)? (2) What are the characteristics of the dynamical evolution of order, correlations, and quantum entanglement in the system?

The first theoretical studies of quenches in quantum many-body systems were performed for the quantum XY and quantum Ising spin chains.¹⁻³ Spectacular experimental results⁴ triggered an intensive research on quantum quenches in various systems such as one-dimensional (1D) Bose systems,⁵⁻⁷ the quantum sine-Gordon model,⁸ Luttinger liquids,⁹ and others.¹⁰ Aside from studies on specific models, there are also field-theoretical investigations, in which relation with boundary critical phenomena and conformal field theory are utilized.¹¹⁻¹³ Progress in understanding thermalization, or absence thereof, in a particularly well-studied integrable model, the transverse Ising chain, has been achieved in Refs. 14 and 15. The concept of an effective temperature depending on the quench parameters is useful to parametrize the relaxation time and correlation length determining the spin correlations after a global quench. But, actually each excitation mode has its own thermalization temperature,¹⁶ implying that the system never thermalizes after a quench.

For the transverse Ising chain in thermal equilibrium, Sachdev and Young¹⁷ introduced a semiclassical description of the equilibrium quantum relaxation in terms of ballistically moving quasiparticles. This description turned out to be surprisingly accurate in predicting the temperature dependence of relaxation time, correlation length, and scaling forms in the ferromagnetic and paramagnetic phases.

For global quantum quenches, a picture of ballistically moving quasiparticles spontaneously created after the quench has been used^{11,18} to explain several features of the time evolution of different quantities, in particular, that of the entanglement entropy.^{19,20} This picture has also been used to interpret results of exact calculations obtained with the free-fermion technique^{14,15} or field theory (at the critical point).^{11,18}

Obviously, it would be desirable to have a quantitative semiclassical theory for the nonequilibrium dynamics after quantum quenches, too. This is what we will present in this paper for global quenches; for local quenches, a brief account has been given by us recently in Ref. 21. Here, we present the quantitative analog of the semiclassical theory for equilibrium quantum relaxation of transverse Ising chains¹⁷ and generalize it to the nonequilibrium dynamics in *finite* systems. By this, we will not only obtain accurate predictions for the relaxation times and correlation lengths, but also about the recurrence times and quasiperiodicity of time-dependent correlations in finite systems with open or periodic boundary conditions. Since in experimental setups of quantum quenches, as for instance cold-atom systems, the number of particles is rather restricted and far away from the infinite system size limit, the understanding of finite-size effects in nonequilibrium quantum relaxation is important and often may be, as we will show, drastic.

The paper is organized as follows: After the model definition in the next section, we present the semiclassical theory for the nonequilibrium dynamics of the transverse Ising chain after a quench. Then, we derive the semiclassical formula for the local magnetization, equal-time bulk-bulk and surface-to-bulk correlations, and bulk autocorrelations and compare the predictions with the results from exact free-fermion calculations. Finally, we discuss the range of applicability of the semiclassical theory and possible generalizations and extensions.

II. MODEL

The system we consider in this paper is the quantum Ising chain defined by the Hamiltonian²²

$$\mathcal{H} = -\frac{1}{2} \sum_{l=1}^{L-1} \sigma_l^z \sigma_{l+1}^z - \frac{h}{2} \sum_{l=1}^L \sigma_l^x \quad (1)$$

in terms of the Pauli matrices $\sigma_l^{x,z}$ at site l . In Eq. (1), the chain has a finite length L and open boundaries; later we will also discuss periodic boundary conditions. (Here, we use such a representation of \mathcal{H} , which is convenient in the ferromagnetic phase, in particular, for $h \ll 1$.) We consider global quenches in which the transverse field strength is suddenly changed from h_0 for $t < 0$ to $h \neq h_0$ for $t > 0$. For $t < 0$, the system is in equilibrium, which means it is in its ground state $|\Psi_0\rangle$ and which we denote as its initial state. After the quench, for $t > 0$, the state $|\Psi_0\rangle$ evolves according to the new Hamiltonian

$$|\Psi_0(t)\rangle = \exp(-i\mathcal{H}t)|\Psi_0\rangle. \quad (2)$$

Similarly, we have for the time evolution of an operator $\sigma_l(t) = \exp(-it\mathcal{H})\sigma_l \exp(it\mathcal{H})$.

We consider the general, time- and space-dependent correlation function

$$C(r_1, t_1; r_2, t_2) = \langle \Psi_0 | \sigma_{r_1}^z(t_1) \sigma_{r_2}^z(t_2) | \Psi_0 \rangle, \quad (3)$$

and study its behavior in special circumstances. The autocorrelation function is obtained for $r_1 = r_2 = r$, which is denoted as $G_r(t_1, t_2)$, whereas for $t_1 = t_2 = t$, we have the equal-time correlation function. This latter quantity for large separation behaves as $C(r_1, t; r_2, t) \equiv C_t(r_1, r_2) = m_{r_1}(t) m_{r_2}(t)$, where $m_r(t)$ is the local magnetization. In the initial state (and in the thermodynamic limit $L \rightarrow \infty$) for $h_0 < h_c = 1$, there is a finite magnetization $m_r(0) > 0$, whereas for $h_0 > 1$ one has $m_r(0) \sim O(1/L)$.

A. Free-fermion representation

The Hamiltonian in Eq. (1) can be expressed in terms of free-fermion creation η_p^\dagger and annihilation operators η_p ^{22,23} as

$$\mathcal{H} = \sum_p \varepsilon_h(p) (\eta_p^\dagger \eta_p - 1/2), \quad (4)$$

where the energy of modes is given by

$$\varepsilon_h(p) = \sqrt{(h - \cos p)^2 + \sin^2 p}. \quad (5)$$

The quasimomenta p has L quasiequidistant values in the interval $0 < p < \pi$ for free boundary conditions, whereas for closed chains, these are restricted to $|p| < \pi$. Time evolution of the fermion operators are $\eta_p^\dagger(t) = e^{it\varepsilon(p)}\eta_p^\dagger$ and $\eta_p(t) = e^{-it\varepsilon(p)}\eta_p$ from which one can obtain the time evolution of the spin operators. The correlation functions in the fermion representations are expressed in terms of Pfaffians, which are then calculated as the square root of the determinant of the corresponding antisymmetric matrix, which has the elements of the Pfaffian above the diagonal. For free boundary conditions, these determinants have a dimension $2(r_1 + r_2)$. Following Yang,²⁴ the local magnetizations can be calculated in the form of an off-diagonal matrix element $m_r(t) = \langle \Psi_0 | \sigma_r^z(t) | \Psi_1 \rangle$, where $|\Psi_1\rangle$ denotes the first excited state for $t < 0$. Its numerical calculation necessitates the solution of a $2r \times 2r$ determinant.

III. SEMICLASSICAL THEORY

In the absence of the transverse field in Eq. (1), $h = 0$, the system is identical with the classical Ising spin chain. The ground state is twofold degenerate and given by $|\Psi_0\rangle =$

$|++++\dots\rangle$ and $|\Psi_0\rangle = |--\dots--\rangle$ and the first excited states are $(L-1)$ fold degenerate given by the single-kink states $|n\rangle = |++\dots+-\dots--\rangle$, where n denotes the kink position. Switching on a small transverse field $h > 0$, the low-lying excitations are, in first-order degenerate perturbation theory, superpositions of these single-kink states $\sum_n a_n |n\rangle$ with excitation energy $\varepsilon_h(p)$. The actual perturbation calculation yields $a_n = \sqrt{2/L} \sin(pn)$, with $\varepsilon_h(p) = 1 - h \cos p$, where p has $L-1$ discrete values in the same region as given below Eq. (5). Thus, the low-lying excitations of \mathcal{H} are Fourier transforms of localized single-kink states, similar to the eigenstates of the Hamiltonian for free particles in a box of length L . Analogously, freely moving single kinks are therefore wave packets of the aforementioned low-lying excitations. Their energy agrees to leading order in h with the free-fermion energies in Eq. (5) and they move ballistically with constant velocity $\pm v_p$ given by

$$v_p = \frac{\partial \varepsilon_p}{\partial p} = \frac{h \sin(p)}{\varepsilon_p}. \quad (6)$$

Ballistically moving kinks are then the (fermionic) quasiparticles (QPs), which we use in the following to formulate a semiclassical theory of the quantum quench dynamics of the transverse Ising model. Since by definition these QPs are well defined at small fields in the ferromagnetic phase, the theory is expected to be applicable for quenches in the ferromagnetic phase. It will turn out that it actually holds in the whole ferromagnetic region not too close to the critical point ($h = 1$). In the paramagnetic phase, one can start with the $h \rightarrow \infty$ ground state to introduce an analogous QP concept involving individual spin flips instead of kinks,¹⁷ but the same dispersion relation (5) and velocity (6). We will mention the necessary modifications below.

Immediately after the quench, the time-dependent state of the system in Eq. (2), which for small h and small t is given by

$$\begin{aligned} |\Psi_0(t)\rangle &\sim \exp\left(-it h \sum_l \sigma_l^x\right) |\Psi_0\rangle \\ &= \prod_l \left[\cos(th) + \iota \sin(th) \sigma_l^x \right] |\Psi_0\rangle. \end{aligned} \quad (7)$$

This indicates that, by the action of the σ_l^x operators, initially single spins are flipped and thus pairs of kinks are created at each lattice point, which then move ballistically with a speed $v \sim h$. The maximum velocity is $v_{\max} \approx h$ for small h .

In a translationally invariant system, the creation probability of QPs is uniform and will be denoted by $f_p(h_0, h)$. For open boundary conditions, there will be corrections to a uniform creation probability close to the boundaries, which are negligible for sufficiently large system sizes. In an equilibrated system that is thermalized at temperature T , this would be $f_p^{\text{eq}}(h_0, h) = e^{-\varepsilon_p/T}$. For zero temperature, quantum relaxation $f_p(h_0, h)$ is the probability with which the modes with momentum number p are occupied in the initial state $|\Psi_0\rangle$, i.e.,

$$f_p(h_0, h) = \langle \Psi_0 | \eta_p^\dagger \eta_p | \Psi_0 \rangle. \quad (8)$$

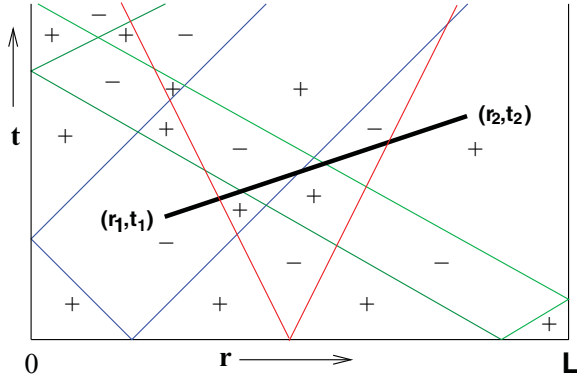


FIG. 1. (Color online) Typical semiclassical contribution to the correlation function $C(r_1, t_1; r_2, t_2)$. Note that the six trajectories of the three QP pairs intersect the line $(r_1, t_1; r_2, t_2)$ five, i.e., an odd number, of times, which implies that $\sigma_{r_1}^z(t_1)$ and $\sigma_{r_2}^z(t_2)$ have opposite orientation. Equivalently, one can say that the trajectories of the red and the green QP pair intersect $(r_1, t_1; r_2, t_2)$ an even number of times (and thus do not contribute) and the trajectory of the blue QP pair an odd number of times.

In a finite system with open boundaries a QP with momentum p moves uniformly with velocity v_p until it reaches one of the boundaries, where it is reflected and moves with velocity $-v_p$ thereafter, and so forth. The trajectory of the kink is periodic in time; after a time $2T_p$ with

$$T_p = L/v_p \quad (9)$$

(including a reflection at the right and left boundaries), it returns to the starting point x_0 with the initial direction and velocity v_p (see Fig. 1). Due to conservation of momenta after a global quench, QPs emerge pairwise at random positions with velocities $+v_p$ and $-v_p$, as indicated in Fig. 1 for three QP pairs.

For a given QP pair created (at $t = 0$) at position $x_0 \in [0, L]$, let $x_1(t)$ be the position of the initially right-moving QP (i.e., with initial velocity v_p) at time t and $x_2(t)$ be the position of the initially left-moving one (i.e., with initial velocity $-v_p$). We define t_a as the time when the left-moving particle reaches the left wall the first time and t_b as the time when the right-moving particle reaches the right wall the first time:

$$t_a = x_0/v_p, \quad t_b = (L - x_0)/v_p. \quad (10)$$

Then, for $t \leq T_p$,

$$x_1(t) = \begin{cases} x_0 + v_p t & \text{for } t \leq t_b, \\ 2L - x_0 - v_p t & \text{for } t_b < t \leq T_p, \end{cases} \quad (11)$$

$$x_2(t) = \begin{cases} x_0 - v_p t & \text{for } t \leq t_a, \\ v_p t - x_0 & \text{for } t_a < t \leq T_p. \end{cases}$$

At $t = T_p$, the two QPs meet at $x = L - x_0$. For $T_p < t < 2T_p$ the trajectories are defined accordingly (see Fig. 2), and for $t > 2T_p$, one notes that x_1 and x_2 are $2T_p$ periodic.

Since QPs represent kinks or domain walls, σ^z changes sign each time a QP passes. Therefore, the correlation function in Eq. (3) can be evaluated in terms of classical particles moving according to (11) by using a similar reasoning as in equilibrium,¹⁷ the difference being that here (1) QP trajectories

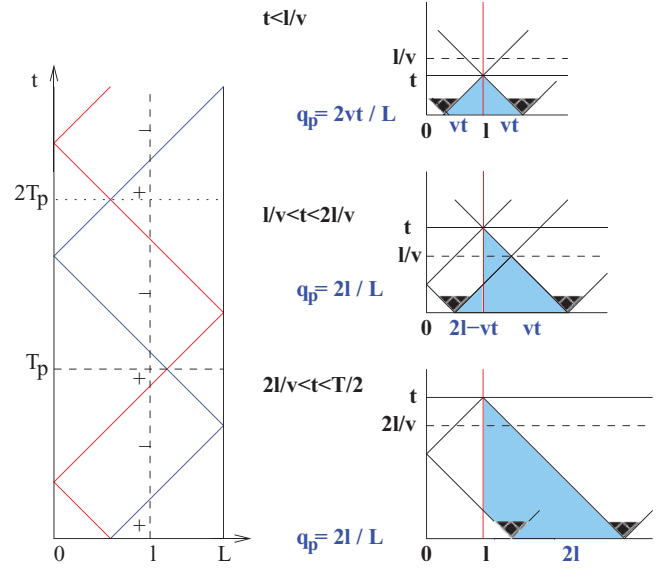


FIG. 2. (Color online) Left: Typical semiclassical contribution to the time dependence of the local magnetization $m_l(t)$. Full lines are quasiparticles or kinks moving with velocity v_p through the chain. The \pm signs denote the sign of the spin at site l . Right: Sketch of the trajectories of kink pairs that flip the spin at position l exactly once for times $t < T_p/2$. Kink pairs with initial position x_0 outside the marked region either do not flip the spin at l (since they do not reach the position l within time t) or they flip it twice. q_p is the fraction of the marked intervals on the $t = 0$ axis.

can intersect the line $(r_1, t_1; r_2, t_2)$ several times, (2) QP trajectories come always in pairs with a common off spring at $t = 0$, and (3) the occupation number of QPs is not thermal.

If a QP trajectory intersects the line $(r_1, t_1; r_2, t_2)$ an odd number of times, the spins at (r_1, t_1) and (r_2, t_2) have the opposite orientations [i.e., $\sigma_{r_1}^z(t_1) = -\sigma_{r_2}^z(t_2)$], which contributes to the decay of the correlation between $\sigma_{r_1}^z(t_1)$ and $\sigma_{r_2}^z(t_2)$ (see Fig. 1). If the two trajectories pass an even number of times, the spins have the same orientation, as if the trajectories did not pass the line $(r_1, t_1; r_2, t_2)$ at all. Let $Q(r_1, t_1; r_2, t_2)$ be the probability that the QPs, which have started from the same site, have passed the line $(r_1, t_1; r_2, t_2)$ a total odd number of times. Then, the probability that for a given set of n sites the kinks have passed (for each site total odd times) this line is $Q^n(1 - Q)^{L-n}$. Summing over all possibilities, we have

$$\frac{C(r_1, t_1; r_2, t_2)}{C_{\text{eq}}(r_1, r_2)} = \sum_{n=0}^L (-1)^n Q^n (1 - Q)^{L-n} \frac{L!}{n!(L-n)!}$$

$$= (1 - 2Q)^L \approx e^{-2Q(r_1, t_1; r_2, t_2)L}, \quad (12)$$

where $C_{\text{eq}}(r_1, r_2)$ is the equilibrium correlation function in the initial state and, in the last step, we have used that the probability $Q(r_1, t_1; r_2, t_2)$ is small. To calculate Q , one should average over the QPs with momenta $p \in [-\pi, \pi]$ or, equivalently, one can average over QP pairs, which is restricted to $p \in [0, \pi]$. In this second method, we have the expression

$$Q(r_1, t_1; r_2, t_2) = \frac{1}{2\pi} \int_0^\pi dp f_p(h_0, h) q_p(r_1, t_1; r_2, t_2) \quad (13)$$

in terms of the occupation probability [see Eq. (8)] and the passing probability $q_p(r_1, t_1; r_2, t_2)$. This latter quantity measures the probability that the two trajectories $x_1(t)$ and $x_2(t)$ of any QP pair with momentum p intersect the line $(r_1, t_1; r_2, t_2)$ together an odd number of times. The same probability for a given QP pair, which is emitted at site $x_0 \in [0, L]$, is denoted by $q_p(x_0 | r_1, t_1; r_2, t_2)$. If we assume that the generation of QPs at the quench is homogeneous in space, then we obtain

$$q_p(r_1, t_1; r_2, t_2) = \frac{1}{L} \int_0^L dx_0 q_p(x_0 | r_1, t_1; r_2, t_2). \quad (14)$$

In most cases of interest (see below), it is possible to provide an analytical form for the function $q_p(r_1, t_1; r_2, t_2)$. If not, the number of intersections can straightforwardly be determined numerically and averaged over x_0 , yielding $q_p(r_1, t_1; r_2, t_2)$ and, thus, $Q(r_1, t_1; r_2, t_2)$ in Eq. (13) and the correlation function in Eq. (3).

IV. LOCAL MAGNETIZATION

The time-dependent local magnetization at a site l (here we consider $l \leq L/2$) can be formally expressed to a correlation between a spin that is fixed at time $t = 0$ (to, say, $\sigma_l^z = +1$) and the same spin at later times t , i.e., $m_l(t) = m_l^{\text{eq}} \cdot C|_{\sigma_l^z(t=0)=+1}(l, 0; l, t)$. Then, with Eq. (3),

$$m_l(t) = m_l^{\text{eq}} e^{-2q(t, l)L} \quad (15)$$

with $q(t, l) = Q|_{\sigma_l^z(t=0)=+1}(l, 0; l, t)$, which is, with Eq. (13),

$$q(t, l) = \frac{1}{2\pi} \int_0^\pi dp f_p(h_0, h) q_p(t, l), \quad (16)$$

where

$$q_p(t, l) = \frac{1}{L} \int_0^L dx_0 q_p(x_0, t, l) \quad (17)$$

as in Eq. (14). To calculate q_p , one concentrates first on times $t < T_p/2 = L/2v_p$. Now, q_p is just the fraction of possible initial positions from which kink pairs can start with velocity $+v_p$ and $-v_p$ that flip the spin at position l exactly once. This region is marked in the sketch of Fig. 2. One sees that, for $t < l/v_p$, one gets $q_p = 2vt/L$, and for $l/v_p < t < T_p/2$, one gets $q_p = 2l/L$, independent of time.

For $T_p/2 < t < T_p$, one observes that a kink pair that started (at $t = 0$) at position x_0 reunites after a time $t = T_p$ at position $L - x_0$. Since the origins of kink pairs are distributed uniformly over the chain, the probability $q_p(t, l)$ is T_p periodic (note: the kink trajectories themselves are only $2T_p$ periodic). Moreover, $q_p(t, l)$ is symmetric with respect to time inversion since it is symmetric under the QP velocity inversion $q_p(-t, l) = q_p(t, l)$, therefore, $q_p(T_p - t, l) = q_p(t, l)$. Defining the reflection times $t_1 = l/v_p$ and $t_2 = T_p - t_1$, one then has, for the period $0 \leq t < T_p$ for $l < L/2$,

$$q_p(t, l) = \begin{cases} 2v_p t/L & \text{for } t \leq t_1, \\ 2l/L & \text{for } t_1 \leq t \leq t_2, \\ 2 - 2v_p t/L & \text{for } t_2 \leq t < T_p. \end{cases} \quad (18)$$

For $l > L/2$, one uses the symmetry $q_p(t, l) = q_p(t, L - l)$ and, for $t > T_p$, one makes use of the T_p periodicity of $q_p(t, l)$:

$$q_p(t + nT_p, l) = q_p(t, l) \quad (n = 1, 2, \dots). \quad (19)$$

Although $q_p(t, l)$ is T_p periodic, $q(t, l)$ is not periodic, since all QPs have different speed. Nevertheless, the maximum speed $v_{\text{max}} = h + O(h^2)$ determines the onset of magnetization reconstruction and, therefore, a quasiperiodicity of $q(t, l)$ and concomitantly $m_l(t)$, the (quasi)period of which is then expected to be

$$T_{\text{period}} = L/v_{\text{max}} \approx L/h. \quad (20)$$

With Eqs. (16), (18), and (19), one obtains $m_l(t)$ via numerical integration (or summation over the discrete p values for a lattice of finite size L).

For an actual calculation, one needs to know the occupation probability $f_p(h_0, h)$ in Eq. (8), which can be calculated numerically in a straightforward manner using the free-fermion technique. Since for large system sizes the occupation probability is not expected to depend strongly on the boundary condition, we will use in the following the expression for $f_p(h_0, h)$ for periodic boundary conditions, which can be given in analytical form as shown in the Appendix [see Eq. (A8)]. In Fig. 3, the prediction of the semiclassical computation is shown. One observes the predicted quasiperiodicity for finite lattices and the expected exponential decays in l and t as discussed below.

In Fig. 4, we compare the semiclassical prediction with the exact results obtained with the free-fermion technique and find that the agreement is remarkably good. We observe that small deviations occur in the bulk ($l \sim L/2$) for $t > T_{\text{period}}/2$, which is when the first QP reflections are involved in the dynamical evolution of $m_l(t)$. For sites close to the boundary, i.e., small l , we observe small deviations already in the plateau region (cf. also the surface-to-bulk correlations discussed further below). Here, a spatially inhomogeneous QP creation probability would have the most significant effect, which is negligible for bulk spins.

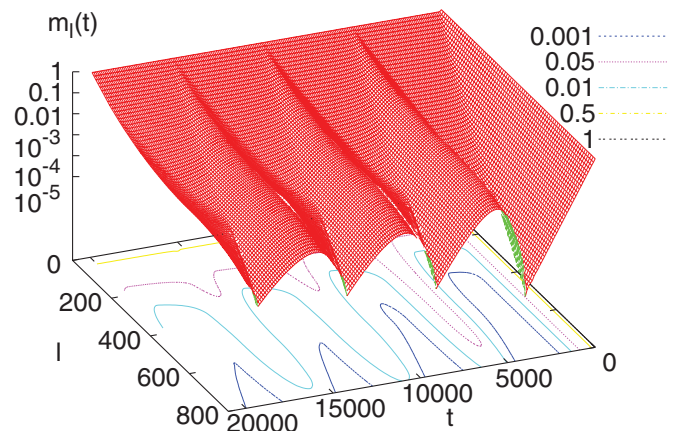


FIG. 3. (Color online) Semiclassical prediction for the local magnetization $m_l(t)$ quench. Here, $L = 1024$, $h_0 = 0$, $h = 0.2$. The (quasi)periodicity (20) is $T_{\text{period}} = L/h = 5120$.

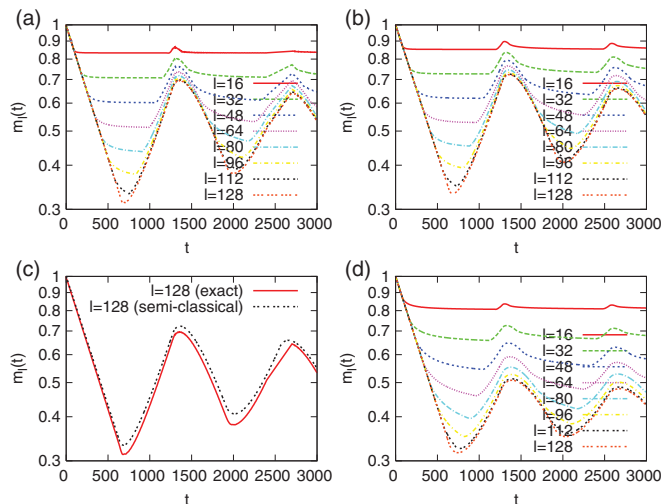


FIG. 4. (Color online) Relaxation of the local magnetization log $m_l(t)$ at different positions in a $L = 256$ chain with free ends after a quench with parameters $h_0 = 0.0$, $h = 0.2$, and $L = 256$. (a) Exact (free-fermion calculation). (b) Semiclassical prediction (15) with the passing probability (18) and the occupation probability (A8). (c) Comparison between exact and QP calculation for $m_l(t)$ for $L = 256$, $l = 128$ for a quench from $h_0 = 0$ to 0.1 . (d) Semiclassical prediction using a thermal occupation number probability in Eq. (21) with an effective temperature T_{eff} (see the text).

When the system after the quench would be thermalized at some effective temperature $T_{\text{eff}}(h_0, h)$,¹⁴ this would imply that the occupation probability is

$$f_p(h_0, h) = e^{-\epsilon_p(h)/T_{\text{eff}}(h_0, h)}. \quad (21)$$

The effective temperature is determined from the condition that the relaxation time in equilibrium $\tau_T(h, T)$ (with transverse field h and temperature T) is the same as in quantum relaxation at $T = 0$, but after a quench from h_0 to h . In the limit $T \ll \Delta(h)$, $\Delta(h)$ being the gap of the system, we have¹⁷ $\tau_T(h, T) \approx \frac{\pi}{2T} e^{\Delta/T}$, which should be compared with $\tau(h_0, h)$, which for small h and h_0 is given in Eq. (39). The result of the semiclassical calculation using (21) is also shown in Fig. 4(d) and compared with the exact data for a quench from $h_0 = 0$ to 0.2 . One sees that, using the proper effective temperature, the initial exponential decay agrees perfectly, but as soon as the first reflections are involved, large deviations occur. An effective temperature can describe the initial relaxation well because essentially it is a fit parameter for the initial exponential decay, which stops after some (l -dependent) time in a finite system.

In the infinite system size limit $L \rightarrow \infty$, the time t_2 in Eq. (18) is infinite for all momenta p . Thus, the (quasi)periodicity of $m_l(t)$ is lost and the functional form of $m_l(t)$ as predicted by (18), (16), and (15) is

$$m_l(t) = m_l^{\text{eq}} \exp\left(-t \frac{2}{\pi} \int_0^\pi dp v_p f_p(h_0, h) \theta(l - v_p t)\right) \times \exp\left(-l \frac{2}{\pi} \int_0^\pi dp f_p(h_0, h) \theta(v_p t - l)\right), \quad (22)$$

which defines, in analogy to¹⁷ the quench-specific length and time scales

$$\begin{aligned} \tau_{\text{mag}}^{-1}(h_0, h) &= \frac{2}{\pi} \int_0^\pi dp v_p f_p(h_0, h), \\ \xi_{\text{mag}}^{-1}(h_0, h) &= \frac{2}{\pi} \int_0^\pi dp f_p(h_0, h). \end{aligned} \quad (23)$$

In the small h and h_0 limits, these are calculated in Eqs. (39) and (32), respectively.

In a finite system, there is a quasiperiodicity and the magnetization after the first relaxation period is reconstructed. Due to the p dependence of the velocity of the QPs in the reconstruction regime, the rate of exponential increase of the magnetization τ'_{mag} is increasing in time. Its maximal value is reached at $t = T_{\text{period}}$, which is given by

$$\begin{aligned} \frac{1}{\tau'_{\text{mag}}(h_0, h)} &= \frac{2}{\pi} \left[\int_{\pi/6}^\pi - \int_0^{\pi/6} \right] dp v_p f_p(h_0, h) \\ &\approx h(h - h_0)^2 \frac{9\sqrt{3} - 8}{12\pi}, \end{aligned} \quad (24)$$

where the second expression is valid in the small h and h_0 limits. One can see that $\tau(h_0, h) < \tau'(h_0, h)$, thus, the reconstruction is slower than the relaxation. While QPs with large energy and high velocity contribute to the reconstruction, the other QPs with smaller energy and lower velocity still reduce the magnetization. These processes with opposite effect are responsible for the decay of the amplitude of the quasiperiodic oscillations of the profile (see Figs. 3 and 4).

After quenches into the disordered phase ($h > 1$), the relaxation (and recurrent) dynamics of the longitudinal magnetization is superposed by oscillations from the ground-state correlations¹⁷ and one has to replace m_l^{eq} in Eq. (15) by

$$m_l^{\text{eq}} \rightarrow m_l^{\text{eq}} K(t\Delta), \quad (25)$$

where $K(x)$ is the modified Bessel function. The results for the corresponding QP calculation and comparison with the exact data are shown in Fig. 5. One observes again that the relaxation and recurrent dynamics is well described by the semiclassical picture also for quenches into the paramagnetic (disordered) phase. The superposed oscillations have a slightly larger amplitude and frequency. Note also that for quenches from the paramagnetic phase [Figs. 5(c) and 5(d)], the equilibrium profiles (m_l^{eq}) shift the curves for $m_l(t)$ downward for increasing l since in the paramagnetic phase, the surface magnetization is larger than the bulk magnetization in a finite chain (both vanishing only in the infinite system size limit).

V. CORRELATION FUNCTIONS

As mentioned before, it is possible to perform the semiclassical calculation for the two-spin correlations $C(r_1, t_1; r_2, t_2)$ for any pair of sites r_1, r_2 and any pair of times t_1, t_2 with the formulas (3), (13), and (14). Here, we want to focus on the time dependence of equal-time correlations between spins separated by a distance r and arranged symmetrically within the bulk, i.e., we consider

$$C_r(r) = C(L/2 - r/2, t; L/2 + r/2, t) \quad (26)$$

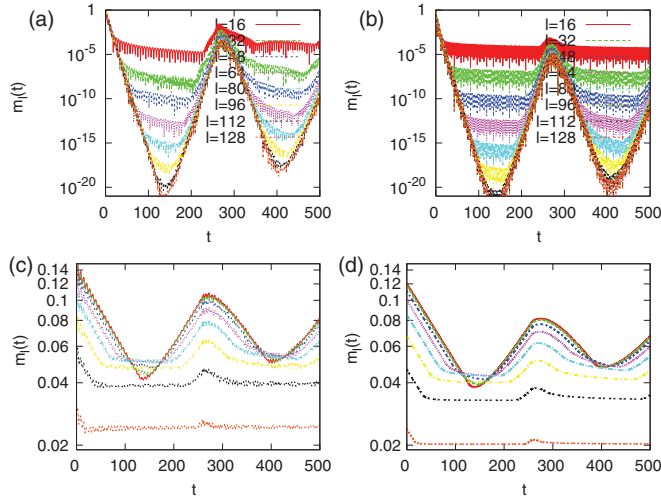


FIG. 5. (Color online) Relaxation of the local magnetization $m_l(t)$ after quenches into the disordered phase, from the ordered phase ($h_0 = 0.5$, $h = 1.5$) (a) exact, (b) semiclassical, and from the disordered phase ($h_0 = 1.5$, $h = 2.0$) (c) exact, (d) semiclassical. The legend of (a) and (b) holds also for (c) and (d), the system size is $L = 256$.

for quenches within the ordered phase ($h < 1$), which is, within the semiclassical theory, given by

$$C_t(r) = C_{\text{eq}}(r) \exp\left(-\frac{L}{2\pi} \int_0^\pi dp f_p(h_0, h) q_p^c(t, r)\right). \quad (27)$$

As sketched in Fig. 6, the function $q_p^c(r, t)$ for $C_t(r)$ is $T_p/2$ periodic, and for the period $0 \leq t < T_p/2$, given by (for $r < L/2$)

$$q_p^c(t, r) = \begin{cases} 4v_p t/L & \text{for } t \leq t_1, \\ 2r/L & \text{for } t_1 \leq t \leq t_2, \\ 2 - 4v_p t/L & \text{for } t_2 \leq t < T_p/2 \end{cases} \quad (28)$$

with $t_1 = r/2v_p$ and $t_2 = T_p/2 - t_1$. (For $r > L/2$, one should replace in the above formulas r to $L - r$.) Note that the relevant times occurring in this expression are all multiplied with a factor $1/2$ as compared to those determining q_p for the local magnetization (18). In particular, $q_p(t, r)$ is $T_p/2$ periodic (in contrast to the T_p periodicity of q_p for the local magnetization): $q_p(t + nT_p/2, r) = q_p(t, r)$ for $n = 1, 2, 3, \dots$. As a result, the (quasi)period of $C_t(r)$ for fixed r is one half of the (quasi)period of the local magnetization $m_l(t)$:

$$T_{\text{period}}^C = L/2v_{\text{max}} \approx L/2h. \quad (29)$$

With (28) and $f_p(h_0, h)$ from the Appendix, the semiclassical calculation can be performed; the results and the comparison with exact data are shown in Figs. 7 and 8.

In Fig. 9, we show the semiclassical prediction for $C_t(r)$ for larger system sizes and long times, scaled by the (quasi)period T_{period}^C [Eq. (29)], which demonstrates the persistence of the recurrence for very long times in finite systems. Note that the recurrence amplitude decreases with increasing system size and vanishes completely for $L \rightarrow \infty$.

In the infinite system size limit $L \rightarrow \infty$, the time t_2 in Eq. (18) is infinite for all momenta p . Thus, the (quasi)periodicity of $C_t(r)$ is lost, and the functional form

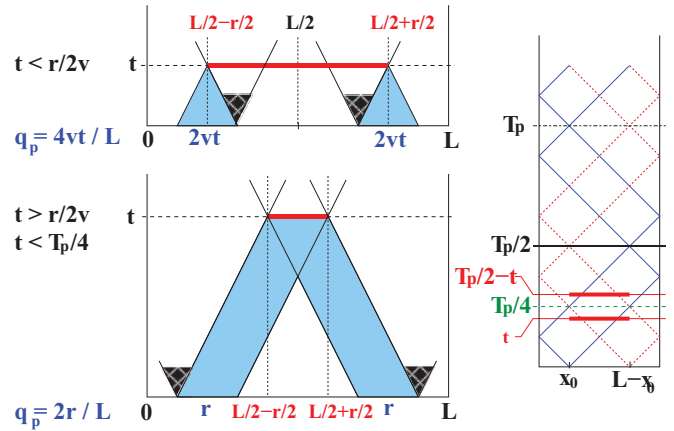


FIG. 6. (Color online) Semiclassical contributions to the equal-time correlation function $C_t(r) = C(L/2 - r/2, t; L/2 + r/2, t)$. Left: Sketch of the trajectories of kink pairs that reverse the orientation of the spins at r_1 and r_2 for times $t < T_p/4$. Kink pairs with initial position x_0 outside the marked region either do not intersect the line ($r_1 = L/2 - r/2, t; r_2 = L/2 + r/2, t$) (red) (since they do not reach the red line within the time t) or they flip it twice. q_p^c is the fraction of the marked intervals on the $t = 0$ axis. Right: Sketch of the additional symmetry of $q_p^c(t)$ that reduce its periodicity from T_p to $T_p/2$. For each QP pair created at position x_0 intersection, the red line at time $t < T_p/4$ there is a QP pair created at position $L - x_0$ that intersects the red line at time $T_p/2 - t$. Hence, $q_p^c(t) = q_p^c(T_p/2 - t)$ for $t < T_p/2$. At $t = T_p/2$, the QP pair created at x_0 meets again at $L - x_0$ and the one created at $L - x_0$ meets again at x_0 , which implies after averaging over initial position that $q_p^c(t + T_p/2) = q_p^c(t)$.

of $C_t(r)$ as predicted by (28) and (27) is

$$C_t(r) = C_{\text{eq}}(r) \exp\left(-t \frac{4}{\pi} \int_0^\pi dp v_p f_p \theta(l - v_p t)\right) \times \exp\left(-r \frac{2}{\pi} \int_0^\pi dp f_p \theta(v_p t - l)\right), \quad (30)$$

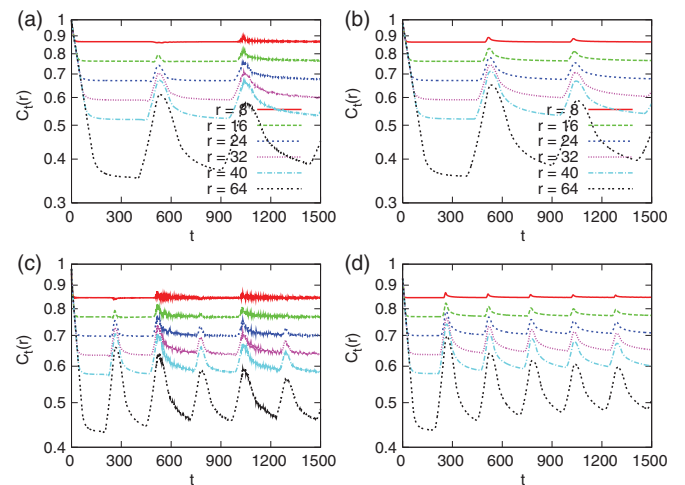


FIG. 7. (Color online) Equal-time correlation function $C_t(r)$ for fixed r as a function of time t after the quench: comparison between the exact result (left) and the semiclassical prediction (right). $L = 256$, $h_0 = 0$, $h = 1.5$ (a) exact, (b) semiclassical; $h_0 = 0.3$, $h = 0.5$ (c) exact, (d) semiclassical. The legend of (a) and (b) holds also for (c) and (d).

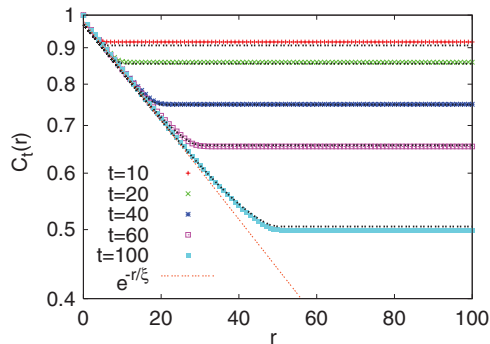


FIG. 8. (Color online) Equal-time correlation function $C_t(r)$ for fixed time t after the quench as a function of distance r : comparison between the exact result (points) and the QP calculation (black broken lines). $L = 256$, $h_0 = 0$, and $h = 0.25$.

with $f_p = f_p(h_0, h)$. This agrees to first order in f_p to the prediction of Ref. 16, where f_p is replaced by $-1/2 \log(1 - 2f_p) = f_p + O(f_p^2)$ (see the Appendix). Equation (30) defines the quench-specific length and time scales

$$\begin{aligned} \tau_c^{-1}(h_0, h) &= \frac{4}{\pi} \int_0^\pi dp v_p f_p(h_0, h), \\ \xi_c^{-1}(h_0, h) &= \frac{2}{\pi} \int_0^\pi dp f_p(h_0, h). \end{aligned} \quad (31)$$

Note that $\tau_c = \tau_{\text{mag}}/2$ and $\xi_c = \xi_{\text{mag}}$. For a small h_0 and h , this yields to leading order

$$\xi_c^{-1}(h_0, h) = \frac{(h - h_0)^2}{2\pi} \int_0^\pi dk \sin^2 k = \frac{(h - h_0)^2}{4}. \quad (32)$$

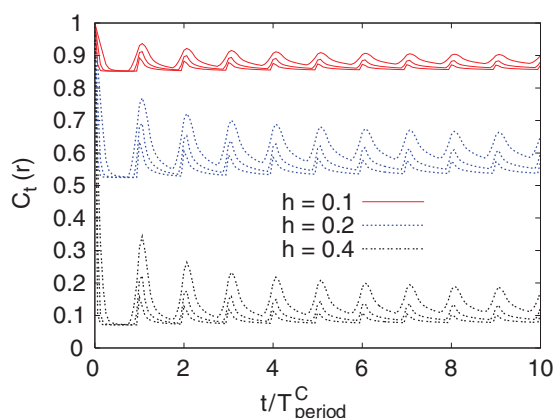


FIG. 9. (Color online) QP prediction for the equal-time correlation function $C_t(r)$ plotted against time after the quench scaled with the (quasi)period $T_{\text{period}}^C = L/2h$ for different fields h ($h_0 = 0$). The three curves for each field h correspond to different system sizes: $L = 256, 512$, and 1024 (from the top curve to the bottom curve).

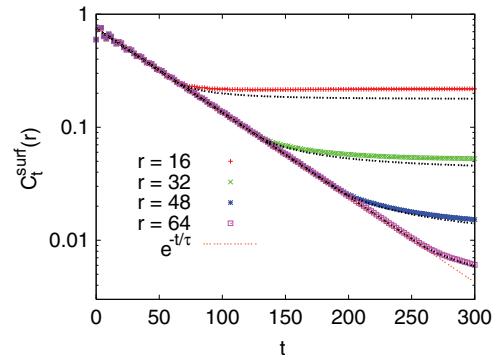


FIG. 10. (Color online) Surface-to-bulk correlation function $C_t^{\text{surf}}(r)$ for fixed time r as a function of the time after the quench. Comparison between the exact result (points) and the QP calculation (black broken lines). $L = 256$, $h_0 = 0.75$, and $h = 0.25$.

A. Surface-to-bulk correlation

The surface-to-bulk correlation function $C_t^{\text{surf}}(r) = C(0, t; r, t)$ is within semiclassical theory given by

$$C_t^{\text{surf}}(r) = C_{\text{eq}}^{\text{surf}}(r) \exp\left(-\frac{L}{\pi} \int_0^\pi dp f_p q_p^{\text{surf}}(t, r)\right) \quad (33)$$

with $f_p = f_p(h_0, h)$. Similar considerations that lead to (18) and (28) yield an analytical expression for $q_p^{\text{surf}}(t, r)$, which is equivalent to $q_p(t, l)$ for the local magnetization in Eq. (18), however, with $l = r$:

$$q_p^{\text{surf}}(t, r) = q_p(t, l = r). \quad (34)$$

Consequently,

$$C_t^{\text{surf}}(r) = C_{\text{eq}}^{\text{surf}}(r) \frac{m_{l=r}(t)}{m_{l=r}^{\text{eq}}}, \quad (35)$$

which implies that the surface-bulk correlation is dominated by the relaxation of the magnetization at the bulk site and that it is T_p periodic [in contrast to $C_t(r)$, which is $T_p/2$ periodic].

In Fig. 10, we show a comparison of this semiclassical result with the exact data. We observe that small deviations occur in the plateau region for small distances r where the bulk correlations still agree very well with the semiclassical prediction. Since for small r both sites in the surface-to-bulk correlation function are close to the boundary, a spatially inhomogeneous QP creation probabilities would have the most significant effects here.

B. Autocorrelations

The autocorrelation function

$$G_l(t) = C(l, 0; l, t) \quad (36)$$

is (up to an extra factor m_l^{eq}) identical to the time-dependent local magnetization $m_l(t)$:

$$G_l(t) = G_{\text{eq}} \frac{m_l(t)}{m_l^{\text{eq}}}. \quad (37)$$

For $l = L/2$ (bulk autocorrelation) in the limit $L \rightarrow \infty$, the QP prediction is

$$G_{L/2}(t) \propto \exp\left(-\frac{2}{\pi} \int_0^\pi dp f_p(h_0, h) \cdot v_p t\right) = e^{-t/\tau_{\text{auto}}} \quad (38)$$

with the relaxation time $\tau_{\text{auto}} = \tau_{\text{mag}}$ [Eq. (23)], which corresponds to the leading order of the result from Calabrese *et al.*¹⁶ (see the Appendix), in which f_p is again replaced by $-1/2 \log(1 - 2f_p) = f_p + O(f_p^2)$. For a small h_0 and h , Eq. (23) yields to leading order

$$\tau^{-1} = \frac{h(h - h_0)^2}{2\pi} \int_0^\pi dk \sin^3 k = h(h - h_0)^2 \frac{2}{3\pi}. \quad (39)$$

This has already been found numerically in Ref. 15.

VI. PERIODIC BOUNDARY CONDITIONS

In a chain with periodic boundary conditions instead of the open boundaries that we considered so far, one has to replace the QP trajectories (11) by the appropriate expressions

$$\begin{aligned} x_1(t) &= (x_0 + v_p t) \bmod L, \\ x_2(t) &= (x_0 - v_p t) \bmod L, \end{aligned} \quad (40)$$

where the modulo operation is defined in the obvious manner: Shift the real number x_i by multiples of L such that it lays in the interval $[0, L]$. With this, the evaluation of the local magnetization and correlation functions is straightforward.

The chain with periodic boundary conditions is translationally invariant, therefore, the equal-time correlation $C_i^{\text{p.b.c.}}(r) = C^{\text{p.b.c.}}(r_1, t_1; r_1 + r, t_2)$ is independent of r_1 . One sees immediately that the expression for $q_p^{\text{p.b.c.}}(t, r)$ is identical to $q_p^c(t, r)$ in Eq. (28), and, therefore, $C_i^{\text{p.b.c.}}(r)$ is identical, up to prefactors from the ground state or equilibrium correlation function, to $C^{\text{open}}(L/2 - r/2, t; L/2 + r/2, t)$:

$$C_i^{\text{p.b.c.}}(r) = \frac{C_{\text{eq}}^{\text{p.b.c.}}(r)}{C_{\text{eq}}^{\text{open}}(r)} C_i^{\text{open}}(r). \quad (41)$$

It should be noted that this relation only holds for the symmetric correlation function $C_i^{\text{open}}(r) = C^{\text{open}}(L/2 - r/2, t; L/2 + r/2, t)$.

The local magnetization $m_l(t)$ is independent of the site l in a system with periodic boundary conditions, as is the QP passing probability $q_p^{\text{p.b.c.}}(t, l) = q_p^{\text{p.b.c.}}(t)$. We find

$$q_p^{\text{p.b.c.}}(t) = \begin{cases} 2v_p t/L & \text{for } t \leq T_p/2, \\ 2 - 2v_p t/L & \text{for } T_p/2 < t \leq T_p. \end{cases} \quad (42)$$

For $t > T_p$, one uses the T_p periodicity $q_p^{\text{p.b.c.}}(t + nT_p) = q_p^{\text{p.b.c.}}(t)$ ($n = 1, 2, \dots$). With Eqs. (15) and (16), the local magnetization is then given by

$$\begin{aligned} \frac{m^{\text{p.b.c.}}(t)}{m_{\text{eq}}^{\text{p.b.c.}}} &= \exp\left(-\frac{2}{\pi} \int_0^\pi dp f_p v_p t \theta[\sin(2\pi t/T_p)] \right. \\ &\quad \left. + \frac{2}{\pi} \int_0^\pi dp f_p (L - v_p t) \theta[-\sin(2\pi t/T_p)]\right). \end{aligned} \quad (43)$$

In the infinite system size limit, this yields

$$m^{\text{p.b.c.}}(t) \propto \exp\left(-t \frac{2}{\pi} \int_0^\pi dp f_p v_p\right) \propto e^{-t/\tau_{\text{mag}}}, \quad (44)$$

which agrees to first order in f_p with the prediction of Ref. 16. As for open boundary conditions, the autocorrelation function $G^{\text{p.b.c.}}(t)$ is given, up to prefactors, by the same expression as the local magnetization (43).

VII. DISCUSSION

We have formulated a semiclassical theory for the nonequilibrium quantum relaxation of the transverse Ising chain after a global quench via an instantaneous change of the transverse field. It is applicable to systems of finite and infinite length and describes properly the relaxation dynamics as well as the recurrence and reconstruction properties of dynamical correlations in finite systems. For infinite systems, our theory agrees to lowest order with a recent prediction by Calabrese *et al.*¹⁶ In particular, the form-factor approach developed in Ref. 16 for the time evolution of the local magnetization leads to results equivalent to our semiclassical theory in Sec. IV. It is expected that other semiclassical theory result, such as those for the correlation function, can be rederived with the form-factor approach.

Our results indicate that the global quantum quench induces a unique length scale ξ and a unique time scale τ in the system, both dependent upon the quench parameters h_0 and h . These characteristic scales appear also in half-infinite geometry and in finite systems, provided the length of the system is larger than ξ . In a finite system, this semiclassical theory not only explains the recurrence and reconstruction properties of the local magnetization,¹⁵ but describes the dynamical behavior quantitatively.

The semiclassical theory can be used to define an effective temperature for the quantum relaxation process. If we compare the expressions obtained by Sachdev and Young¹⁷ for the correlation length and the relaxation time in equilibrium at finite temperatures with our results for zero-temperature quantum quenches, one obtains a node-dependent effective temperature $T_{\text{eff}}(p)$, defined by the condition

$$f_p(h_0, h) = \exp\left(-\frac{\varepsilon_h(p)}{T_{\text{eff}}(p)}\right). \quad (45)$$

This relation agrees to first order in f_p with the prediction of Ref. 16 (i.e., for small effective temperatures or small h and h_0). In Ref. 16, the Boltzmann factor on the right-hand side of Eq. (45) is replaced by the Fermi function with zero chemical potential, as shown in the Appendix in Eq. (A11), thus replacing classical kinks simply by free fermions.

It is interesting to notice an analogous expression for the time evolution of the entanglement entropy $S(t)$, measured after the quench between two semi-infinite parts of the system, say \mathcal{A} and \mathcal{B} . The analytical result by Fagotti and Calabrese¹⁹ can be written into the form

$$S(t) = t \frac{1}{\pi} \int_0^\pi dp v_p s_p(h, h_0), \quad (46)$$

with

$$s_p(h, h_0) = -(1 - f_p) \ln(1 - f_p) - f_p \ln f_p \quad (47)$$

being the entropy of the fermionic mode with occupation number $f_p(h_0, h)$. In the semiclassical theory, this expression can be interpreted as the result of ballistically moving QP pairs, which are created say at \mathcal{A} at $t = 0$ and one of them is reaching \mathcal{B} before the actual time t . Each of these QPs brings an entropic contribution as a free fermion. It would be interesting to see if the relations in Eqs. (A11) and (46) are valid for another integrable quantum spin system, too.

The semiclassical approach is accurate if the occupation probability $f_p(h_0, h)$ is small, which is valid if the initial and the finite states are close to each other and both are ferromagnetic. As shown in Ref. 15 for $h, h_0 < 1$, the magnetization profile $m_l(t)$ for any finite l and t is non-negative. In the other domains of the quench (h_0 and/or h is larger than 1), during relaxation $m_l(t)$ takes negative values, too. This type of oscillating relaxation is described qualitatively well by the semiclassical theory. The amplitude of the oscillations as well as the recurrence of the magnetization and the correlations are correctly described, but there are differences in the actual value of the frequencies. For quenches close to the critical point, we expect the concept of isolated QPs to become invalid or at least quantitatively inaccurate due to the diverging correlation length either in the initial and/or final state.

In the finite system with open boundaries and for half-infinite systems, we find small deviations between the exact and the semiclassical results either when sites close to the boundaries are involved or for times $t > T_{\text{period}}/2$, when QPs reflected at the boundaries contribute to the magnetization or correlation reconstruction. A possible source for the deviations in the first case is the lack of translational invariance in chains with open boundaries, which results in spatially inhomogeneous creation probability of QP pairs, at least close to the boundaries. The second kind of deviations could originate in the dynamical processes during the reflection at the open boundaries, which might be more complicated than just momentum inversion. Both effects are absent in systems without boundaries, the reason for which we expect our predictions to be accurate for all times in finite chains with periodic boundary conditions.

Our semiclassical theory can be generalized in several directions. This theory is also valid for transverse Ising chains involving a sum over more ferromagnetic short-range interactions than only nearest neighbors, as has been argued for the equilibrium relaxation dynamics at finite temperatures by Sachdev and Young.¹⁷ The semiclassical theory should be applicable to nonintegrable models, too, for which one has to include QP collision and scattering processes. Here, the quantum Boltzmann equation seems to be a promising approach,²⁵ as has been demonstrated recently for a bosonic system in Ref. 26.

ACKNOWLEDGMENTS

This work was supported by the Deutsche Forschungsgemeinschaft (DFG) and by the Hungarian National Research Fund under Grants No. OTKA K62588, No. K75324, and No. K77629 and by a German-Hungarian exchange program (DFG-MTA).

APPENDIX

Here, we compare our semiclassical calculation with the predictions by Calabrese *et al.*¹⁶ First, we recapitulate the exact solution of the free-fermion representation, the Hamiltonian in Eq. (4), for periodic boundary conditions. In this case, there are pairs of fermions with quasimomenta p and $-p$, and in the ground-state sector, these are $p = \frac{\pi}{L}, \frac{3\pi}{L}, \frac{5\pi}{L}, \dots, 0 < p < \pi$. Here, we define the functions

$$u_h(p) = \sqrt{\frac{\varepsilon_h(p) + h - \cos p}{2\varepsilon_h(p)}}, \quad (A1)$$

$$v_h(p) = \sqrt{\frac{\varepsilon_h(p) - (h - \cos p)}{2\varepsilon_h(p)}},$$

and

$$U_p = u_{h_0}(p)u_h(p) + v_{h_0}(p)v_h(p), \quad (A2)$$

$$V_p = u_{h_0}(p)v_h(p) - v_{h_0}(p)u_h(p) \quad (A3)$$

in terms of which the ground state for $t < 0$ ($|\Psi_0\rangle$) is expressed with the ground state at $t > 0$ ($|0\rangle$) as

$$|\Psi_0\rangle = \prod_p [U_p + iV_p\eta_p^\dagger\eta_{-p}^\dagger]|0\rangle. \quad (A4)$$

Then, the density of quasiparticle excitations is given by the nonequilibrium occupation number

$$f_p = \langle\Psi_0|\eta_p^\dagger\eta_p|\Psi_0\rangle = |V_p|^2. \quad (A5)$$

This can be expressed as

$$f_p = \frac{1}{2}[1 - \cos \Delta_p], \quad (A6)$$

where Δ_p is the difference between the Bogoliubov angles diagonalizing $\mathcal{H}(h)$ and $\mathcal{H}(h_0)$, respectively:

$$\cos \Delta_p = \frac{h_0h - (h_0 + h)\cos p + 1}{\varepsilon_{h_0}(p)\varepsilon_h(p)}. \quad (A7)$$

For small h_0 and h , we obtain, in leading order for the occupation number,

$$f_p = \frac{1}{4}(h - h_0)^2 \sin^2 p. \quad (A8)$$

The results by Calabrese *et al.*¹⁶ can be formally obtained from our semiclassical expressions if an effective occupation number is used. For example, in Eq. (32) for the correlation length and in Eq. (39) for the relaxation time, one should simply replace

$$f_p \rightarrow -\frac{1}{2} \ln |\cos \Delta_p|. \quad (A9)$$

The semiclassical results then represent the leading term of the exact expressions.

According to Calabrese *et al.*,¹⁶ there is an effective thermal (Gibbs) distribution or generalized Gibbs ensemble (GGE), which is obtained in integrable models by maximizing the entropy, while keeping the energy and other conservation laws fixed. This leads to an effective, node-dependent temperature $T_{\text{eff}}(p)$, which is given by

$$\cos \Delta_p = \tanh \frac{\varepsilon_h(p)}{2T_{\text{eff}}(p)}, \quad (A10)$$

or expressed with f_p , we have

$$f_p = \frac{1}{\exp\left(\frac{\varepsilon_h(p)}{T_{\text{eff}}(p)}\right) + 1}. \quad (\text{A11})$$

At the right-hand side, we have the Fermi distribution function with zero chemical potential, thus, the GGE condition is expressed in the form that the nonequilibrium occupation number of the given mode is equal to its thermal occupation at the effective temperature $T_{\text{eff}}(p)$.

*h.rieger@mx.uni-saarland.de

†igloi@szfki.hu

¹E. Barouch and B. McCoy, *Phys. Rev. A* **2**, 1075 (1970); **3**, 786 (1971); **3**, 2137 (1971).

²F. Iglói and H. Rieger, *Phys. Rev. Lett.* **85**, 3233 (2000).

³K. Sengupta, S. Powell, and S. Sachdev, *Phys. Rev. A* **69**, 053616 (2004).

⁴M. Greiner, O. Mandel, T. W. Hänsch, and I. Bloch, *Nature (London)* **419**, 51 (2002); L. E. Sadler, J. M. Higbie, S. R. Leslie, M. Vengalattore, and D. M. Stamper-Kurn, *ibid.* **443**, 312 (2006); A. Lamacraft, *Phys. Rev. Lett.* **98**, 160404 (2007); B. Paredes *et al.*, *Nature (London)* **429**, 277 (2004); T. Kinoshita, T. Wenger, and D. S. Weiss, *Science* **305**, 1125 (2004); *Nature (London)* **440**, 900 (2006).

⁵M. Rigol, V. Dunjko, V. Yurovsky, and M. Olshanii, *Phys. Rev. Lett.* **98**, 50405 (2007).

⁶C. Kollath, A. M. Läuchli, and E. Altman, *Phys. Rev. Lett.* **98**, 180601 (2007).

⁷G. Roux, *Phys. Rev. A* **79**, 021608(R) (2009).

⁸V. Gritsev, E. Demler, M. Lukin, and A. Polkovnikov, *Phys. Rev. Lett.* **99**, 200404 (2007).

⁹M. A. Cazalilla, *Phys. Rev. Lett.* **97**, 156403 (2006).

¹⁰S. R. Manmana, S. Wessel, R. M. Noack, and A. Muramatsu, *Phys. Rev. Lett.* **98**, 210405 (2007).

¹¹P. Calabrese and J. Cardy, *Phys. Rev. Lett.* **96**, 136801 (2006); *J. Stat. Mech.: Theory Exp.* (2007) P06008.

¹²S. Sotiriadis and J. Cardy, *J. Stat. Mech.: Theory Exp.* (2008) P11003; *Phys. Rev. B* **81**, 134305 (2010).

¹³A. Gambassi and P. Calabrese, *Europhys. Lett.* **95**, 66007 (2011).

¹⁴D. Rossini, A. Silva, G. Mussardo, and G. E. Santoro, *Phys. Rev. Lett.* **102**, 127204 (2009); D. Rossini, S. Suzuki, G. Mussardo, G. E. Santoro and A. Silva, *Phys. Rev. B* **82**, 144302 (2010).

¹⁵F. Iglói and H. Rieger, *Phys. Rev. Lett.* **106**, 035701 (2011).

¹⁶P. Calabrese, F. H. L. Essler, and M. Fagotti, *Phys. Rev. Lett.* **106**, 227203 (2011).

¹⁷S. Sachdev and A. P. Young, *Phys. Rev. Lett.* **78**, 2220 (1997).

¹⁸P. Calabrese and J. Cardy, *J. Stat. Mech.: Theory Exp.* (2005) P04010.

¹⁹M. Fagotti and P. Calabrese, *Phys. Rev. A* **78**, 010306(R) (2008).

²⁰V. Eisler, F. Iglói, and I. Peschel, *J. Stat. Mech.* P02011 (2009).

²¹U. Divakaran, F. Iglói, and H. Rieger, e-print [arXiv:1105.5317](https://arxiv.org/abs/1105.5317).

²²P. Pfeuty, *Ann. Phys. (NY)* **57**, 79 (1970).

²³E. Lieb, T. Schultz, and D. Mattis, *Ann. Phys. (NY)* **16**, 407 (1961).

²⁴C. N. Yang, *Phys. Rev.* **85**, 808 (1952).

²⁵J. M. Ziman, *Electrons and Phonons* (Oxford University Press, New York, 1960).

²⁶U. Schneider *et al.*, e-print [arXiv:1005.3545](https://arxiv.org/abs/1005.3545).